Suggested Citation format for this article:

Silva, Luis F. O., Oliveira, Marcos L. S., Kautzmann, Rubens M., Ramos, Claudete G., Izquierdo, Maria, Dai, Shifeng, Wilcox, Jennifer, Hoffman, Jeremy, Hower, James C., 2014, Geochemistry and Mineralogy of Coal-Fired Circulating Fluidized Bed Combustion Fly Ashes. *Coal Combustion and Gasification Products* 6, 6-28, doi: 10.4177/CCGP-D-14-00005.1

Geochemistry and Mineralogy of Coal-Fired Circulating Fluidized Bed Combustion Fly Ashes

Luis F.O. Silva[1,2], Marcos L.S. Oliveira[3], Rubens M. Kautzmann[1], Claudete G. Ramos[1], Maria Izquierdo[4], Shifeng Dai[5], Jennifer Wilcox[6], Jeremy Hoffman[6], James C. Hower[7,*]

[1] Laboratory of Environmental Researches and Nanotechnology Development, Centro Universitário La Salle, Mestrado em Avaliação de Impactos Ambientais em Mineração, Victor Barreto, 2288 Centro, 92010-000 Canoas, RS, Brazil
[2] Environmental Science and Nanotechnology Department, Catarinense Institute of Environmental Research and Human Development – IPADHC, Capivari de Baixo, Santa Catarina, Brazil
[3] Development Department of Touristic Opportunities, Catarinense Institute of Environmental Research and Human Development – IPADHC, Capivari de Baixo, Santa Catarina, Brazil
[4] School of Applied Sciences, Cranfield University, Cranfield, Bedfordshire MK43 0AL, UK
[5] China University of Mining & Technology, Haidian, Beijing, China
[6] Department of Energy Resources Engineering, Stanford University, Stanford, CA 94305-2220, USA
[7] Center for Applied Energy Research, University of Kentucky, 2540 Research Park Drive, Lexington, KY 40511, USA

ABSTRACT

The fuel, bed ash, and fly ash were sampled from a circulating fluidized bed combustion (CFBC) unit at two times. The first sampling was a high-sulfur (S) coal-only run, and the second sampling coincided with an experimental burn of up to 10% switchgrass (*Panicum virgatum*) pressed pellets mixed with a high-S coal. The latter blend had a higher moisture content and a lower heating value than the coal-only fuel. Given the time between the samplings and the special needs for the experimental run, unavoidable changes in the coal and limestone complicate comparisons of the bed ash and fly ash chemistry between the sampling times. The bed ash is dominated by CaO and SO_3, and the fly ash has a higher CaO content than would be expected for a pulverized-coal burn of the same coal. The fly ash chemistry bears a superficial resemblance to class C fly ashes, but given the different combustion conditions and consequent differences in the ash mineralogy, the fly ash should not be considered to be a class C ash. The bed ash mineral assemblages consist of anhydrite, mullite, portlandite, and anorthite, while the fly ash has less portlandite and more anorthite than the bed ash.

1. Introduction

Power generation worldwide is still heavily reliant on coal combustion, despite the great efforts for renewable power to account for a significant share of the total power generation. With growing energy demand, all energy resources may need to be utilized, and biomass and inexpensive fuels are likely to become increasingly important.

Circulating fluidized bed combustion (CFBC) technology has great fuel flexibility due to a unique combustion and heat-transfer environment (Basu, 1999). CFB boilers can burn even the worst grade of available fuels without any major performance penalty (Basu and Fraser, 1991). Thus, with the increase in waste

* Corresponding author. *Tel.*: 859-257-0261. *E-mail*: james.hower@uky.edu

production, CFBC is playing an important role in (co-)firing secondary fuels that would be disposed of otherwise, e.g., biomass (Cui and Grace, 2007), sludge (Van de Velden et al., 2007), petroleum coke (Chen and Lu, 2007), or even municipal solid waste (Wheeler et al., 1995), in addition to high-ash or high-sulfur (S) coals that would not routinely be considered in pulverized-coal combustion (Kitto and Stultz, 2005).

CFBC utilizes limestone as a sulfur sorbent. Consequently, the sulfur is discharged as a part of a solid residue instead of leaving the boiler as gaseous emissions (Basu, 1999). The combustion temperature of CFBC is about 730–900°C (significantly lower than the 1400–1500°C of a pulverized-coal-combustion boiler), which reduces NO_x formation. The utility CFBC unit studied was built to supply needed generating capacity to the utility's fleet of plants, and the choice of boiler was made in anticipation of stricter U.S. Environmental Protection Agency SO_2-emission controls (US EPA, 2010, 2011). The 268-MW CFBC unit is paired with downstream scrubbers and selective noncatalytic reduction (SNCR) to obtain very low emissions of SO_2 and NO_x (Kitto and Stutz, 2005; Treff and Johnson, 2005).

One of the ways to potentially decrease CO_2 emissions from coal-fired power plants is to co-fire biomass with coal. In 2008, only 4.2 GW of electricity was produced from biomass in the United States, compared with the 313.3 GW of power generated by coal (U.S. Energy Information Administration, 2010). However, co-firing small amounts of biomass with coal has potential for decreasing CO_2 emissions with little loss of electrical output. One of the samples for this study, switchgrass, *Panicum virgatum,* is a U.S. native C4 grass. The C4 grasses are warm-weather species that are able to thrive in hot and dry conditions; they have low nutrient requirements and relatively high calorific value (16.93 MJ/kg).

The main objectives of the present study were to understand mineral matter occurrence in the CFBC ashes, with and without co-fired switchgrass, by using recently developed conventional and advanced nanoscale mineral and petrographic analyses; to investigate the nature and abundance of the glass phases present in fluidized bed combustion (FBC) coal ashes; and to integrate the results in the evaluation of the chemical and mineralogical distributions and of the textural characteristics of ashes, in particular the submicron particles.

2. Materials and Methods

2.1. Sampling

Feed coal, bed ash, and fly ash sampling was conducted at a Kentucky 268-MW CFBC unit in September 2007 by U.S. Geological Survey (USGS) and University of Kentucky Center for Applied Energy Research (CAER) personnel. A second round of sampling, coinciding with a test burn of switchgrass + coal, was conducted in March 2010 by USGS, CAER, and Morehead State University personnel. The ash-collection system consists of two hoppers for the bed ash, also known as the spent bed, and two rows of four baghouse hoppers each for the fly ash collection. The second row, the "out" hoppers, generally has much smaller amounts of fly ash than the first, or "in," row. In some cases for this and previous samplings, no ash could be collected from some of the second-row hoppers. For both collections, with the exception of the March 2010 coal and switchgrass provided by

company officials, the feed fuel, the bed ash from the bottom of the CFBC unit, and each available hopper of the first row of fly ash hoppers were collected in 3.79-L (1-gallon) cans, sealed, and returned to the CAER for crushing (as appropriate) and splitting for distribution to the laboratories.

2.2. Mineralogy, petrology, and particle analysis

Petrographic analyses were performed at the CAER on epoxy-bound particulate pellets, polished to a 0.05-µm alumina final polish, and examined using reflected white-light, oil-immersion optics at a final magnification of 500×. Maceral analyses are reported on a mineral-included and mineral-free basis.

The crystalline mineralogy of ashes was evaluated by X-ray powder diffraction (XRD) on a Philips powder diffractometer fitted with Philips "PW1710" control unit, Vertical Philips "PW1820/00" goniometer, and FR590 Enraf Nonius generator at the Unidade de Raios X - RIAIDT of University of Santiago de Compostela (Spain). The instrument was equipped with a graphite diffracted beam monochromator and copper radiation source (λ[Kα1] = 1.5406 Å), operating at 40 kV and 30 mA. The XRD pattern was collected by measuring the scintillation response to Cu Kα radiation versus the 2Θ value over a 2Θ range of 2–65, with a step size of 0.02° and counting time of 3 seconds per step. The semiquantification of the individual crystalline phases (minerals) in each samples was determined using the program Match! (CRYSTAL IMPACT, Bonn, Germany). The ash samples did not need any treatment prior to analysis measurements. Moreover, the sample was spun during the data collection in order to get the best peak profile and to minimize the preferred orientation effect.

Raman spectroscopy; field emission scanning electron microscopy (FE-SEM); and high-resolution transmission electron microscope (HR-TEM) with selected area electron diffraction (SAED) and/or microbeam diffraction (MBD), scanning transmission electron microscopy (STEM), and energy-dispersive X-ray spectrometer (EDS) analyses were conducted following the procedure reported in our previous studies (Ribeiro et al., 2010; Silva et al., 2011a,b,c; Oliveira et al., 2012; Quispe et al., 2012).

In order to understand nanomineral assemblages, sequential extraction and magnetic separation were conducted following methods reported by Silva et al. (2012). However, only two-dimensional information is available with those techniques. For this reason, in the present research, we used a dual-beam focused ion beam (FIB), the FEI DualBeam^{TM} Helios 600 Nanolab^{TM}, equipped with the following primary components: (1) a high-resolution field emission gun (FEG) for SEM; (2) multiple electron detectors for image acquisition, such as through-the-lens detector (TLD), an Everhart-Thornley detector (ETD), and a backscattered electron detector (BSED) for compositional information; and (3) a high-resolution focused Ga$^+$ ion beam to precisely select, slice, and image a specific region of the species of interest, with a spatial resolution within the 10-nm range. FIB-SEM is an analytical technique based on the unique combination of an ion gun and an electron gun, where specimens can be positioned at the intersection point of the electron and ion beam with an accuracy of much less than 1 µm. This permits simultaneous ion-milling nanosectioning and secondary electron imaging of the region of interest with a spatial resolution within the nanometer range (Giannuzzi et al., 1999). The FIB technique was used to prepare fluidized bed combustion ashes for HR-TEM.

Table 1
Chemistry of samples from the March 2010 collection

MA number	62359	62382	62385	62386	SP-CCS	SP-BC	SP-SP	SP-BAB	SP-B1FAi	SP-B2FAi
Sampling	2007	2007	2007	2007	2010	2010	2010	2010	2010	2010
Sample ID	93548	93550	93553	93554	93582			93585	93588	93589
Sample type	Coal	Bed ash	Fly ash	Fly ash	Coal/switchgrass	Barge coal	Switchgrass pellets	Bed ash B	Fly ash	Fly ash
Bin/hopper	H	B	B1 in	B2 in				CCP bed ash B	CCP fly ash B1 in	CCP fly ash B2 in
%Ash	19.90	98.50	89.65	89.65	19.36	19.50	2.35			
%Moisture	3.33	dl	0.59	0.62	8.01	7.36	11.97	2.10	6.47	6.18
%VM	33.37				31.20	30.20	72.74	2.02	6.70	6.61
%FC	43.40				41.43	42.94	12.94	2.02	6.70	6.61
HV (MJ/kg)	26.02				24.41	24.74	16.93			
%C	61.25	0.68	4.43	4.39	58.55	59.14	42.91			
%H	4.62	0.09	0.41	0.42	3.99	3.92	5.17			
%N	1.04	dl	0.05	0.06	1.13	1.16	0.30		4.90	5.59
%S	3.31	9.07	6.75	6.76	3.24	3.09	<0.6			
%O	9.88	dl	dl	dl				8.66	4.9	5.59
%SiO_2	49.38	15.70	24.84	24.81	52.60	56.60	39.50	20.80	30.20	30.00
%Al_2O_3	20.68	5.98	10.21	10.16	22.20	22.10	2.05	7.42	12.10	12.20
%Fe_2O_3	19.79	2.62	8.47	8.40	15.60	14.70	2.97	5.71	9.11	9.16
%CaO	1.31	54.13	30.60	30.72	0.82	0.65	17.10	41.10	28.00	29.40
%MgO	0.94	1.95	4.64	4.62	0.75	0.72	4.40	1.34	1.26	1.36
%Na_2O	0.26	0.26	0.31	0.31	0.18	0.19	0.61	0.07	0.11	0.11
%K_2O	2.61	0.59	1.21	1.19	2.12	2.1	12.7	1.00	1.21	1.20
%P_2O_5	0.14	0.07	0.08	0.08	0.11	0.12	3.73	0.11	0.09	0.10
%TiO_2	1.10	0.26	0.40	0.39	1.04	1.05	0.14	0.33	0.57	0.57
%SO_3	1.40	20.87	20.80	20.86	0.98	0.78	2.68	26.80	19.30	18.70
As	129	82	62	62	152	116	1.14	69	56	56
Ba	1611	dl	315	298	677	698	868	226	389	386
Be					12	13.1	1.68	4	6	6
Bi					1.34	1.26	0.172	0.65	0.64	0.70
Cd	dl	dl	dl	dl	0.42	0.322	1.27	dl	dl	dl
Cl	473				214	714	277	124		
Co	59	dl	16	16	30	29.9	8.41	15	18	18
Cr	106.00	18	25	44	151	151	41.6	51	67	64
Cs					7	7.43	1.68	3	4	4
Cu	1	dl	dl	dl	102	105	136	44	59	56
F					dl	53	dl	dl		
Ga	0.31				37	37.9	3.32	12	19	19
Ge	n.d.				8	8.66	1.61	7	5	5
Hg (whole ash)		0.01	0.85	0.82	0.24					
Li	473				187	198	66.4	46	87	80
Mn	308	22	70	73	218	179	3080	664	422	489
Mo	12	dl	dl	dl	20	19.4	33.7	5	7	8
Nb					16	16.8	3.95	5	8	8
Ni	62	dl	7	9	61	60.5	34.3	30	33	33
Pb	dl	29	28	29	50	51.5	131	14	30	28
Rb	dl	243	132	162	129	123	89.2	50	64	61
Sb	7	15	11	13	3			1	1	1
Se	n.d.		13.81	13.89	6					
Sr	486	127	193	172	333	335	390	203	261	266
Th					24	24.3	2.41	6	8	8
Tl					8	6.85	1.82	1	3	3

Table 1
Continued

MA number	62359	62382	62385	62386	SP-CCS	SP-BC	SP-SP	SP-BAB	SP-B1FAi	SP-B2FAi
Sampling	2007	2007	2007	2007	2010	2010	2010	2010	2010	2010
Sample ID	93548	93550	93553	93554	93582			93585	93588	93589
Sample type	Coal	Bed ash	Fly ash	Fly ash	Coal/switchgrass	Barge coal	Switchgrass pellets	Bed ash B	Fly ash	Fly ash
Bin/hopper	H	B	B1 in	B2 in				CCP bed ash B	CCP fly ash B1 in	CCP fly ash B2 in
U		dl	dl	dl	7	7.45	1.22	3	4	4
V	268	dl			175	179	24.5	65	90	89
Y					48	49.4	7.16	19	31	29
Zn	58	dl	19	21	87	115	759	254	120	131
Zr	133	221	197	201						

Note: Analyses were done by the University of Kentucky Center for Applied Energy Research (CAER), U.S. Geological Survey (USGS), and Geochemical Testing. Proximate, ultimate analyses, and heating value are on an as-received basis. Major oxides (%) are on ash basis. Minor elements are in parts per million on ash basis, with the exception of Hg, which is on a whole-sample basis. n.d. = not determined; dl = detection limit.

2.3. Chemical characterization

Basic analyses were made in the laboratories of the USGS (following procedures outlined by Meier et al., 1996) and at CAER and are reported here as Table 1. Proximate and ultimate analyses were conducted on LECO equipment following the appropriate ASTM standards at CAER. Mercury analysis was performed at CAER on a LECO AMA-254 Hg analyzer.

The samples were acid digested following a two-step method devised to retain volatile elements (Querol et al., 1997). The process involved a hot HNO_3 extraction, followed by HF-HNO_3-$HClO_4$ digestion of the residue. The resulting solutions were analyzed by inductively coupled plasma–atomic emission spectrometry (ICP-AES) and inductively coupled plasma–mass spectrometry (ICP-MS) for a range of major and trace elements. An international coal reference material (SARM-19) and blanks were also digested and analyzed following the same procedure. This was done in order to check the accuracy of the analytical and digestion methods. Analytical errors were estimated at 3% for most of the elements and around 10% for Cd, Mo, and P.

In order to study the leaching of elements, the compliance leaching test EN 12457-2 (European Committee for Standardisation, 2002) was applied. This is a single-batch leaching test performed at a liquid-to-solid ratio (L/S) of 10 L/kg with 24 hours agitation time and deionized water as leachant. In all cases, analyses were performed in duplicate. Major, minor, and trace element concentrations in solid samples and leachates were determined by means of ICP-MS, ICP-AES, and high-performance liquid chromatography.

3. Results and Discussion

3.1. Petrology

The coal component of the coal + switchgrass blend is dominated by vitrinite-group macerals, as with the mixture of vitrinite and fusinite on Figure 1A, as expected for a central Appalachian coal. Pyrite filling the lumens in fusinite is illustrated in Figure 1B. The switchgrass is shown on white-light (Figure 1C) and blue-light (Figure 1D) images.

3.2. Chemical composition

The feed fuels, coal, and coal + switchgrass are similar with respect to the major oxide and trace element compositions (Table 1). The coal + switchgrass blend has a higher moisture content and lower heating value than the September 2007 feed coal. It must be emphasized that the coal source changed between the two samplings, complicating rigorous comparisons between the two fuels.[1] For this plant, the company informed us that the limestone is from the Silurian Brassfield Formation (with an average of 91.25% $CaCO_3$, 2.12% $MgCO_3$, and 4.32% SiO_2).

The switchgrass, while having about one-third less heating value than the coal, is much lower in ash yield and sulfur content (Table 1). Fuel for CFBC boilers is generally selected due to its relatively high-ash and high-S content, basically, coals that would not necessarily be selected for pulverized-coal combustion. Therefore, the low ash and S contents of the switchgrass are not the reason for its use in a CFBC. Rather, the use of a low-cost renewable fuel, the offset of coal-fired

[1] Broad coal-related differences in fly ash characteristics were discussed in Hower et al. (1996, 1999a,b, 2005, 2009).
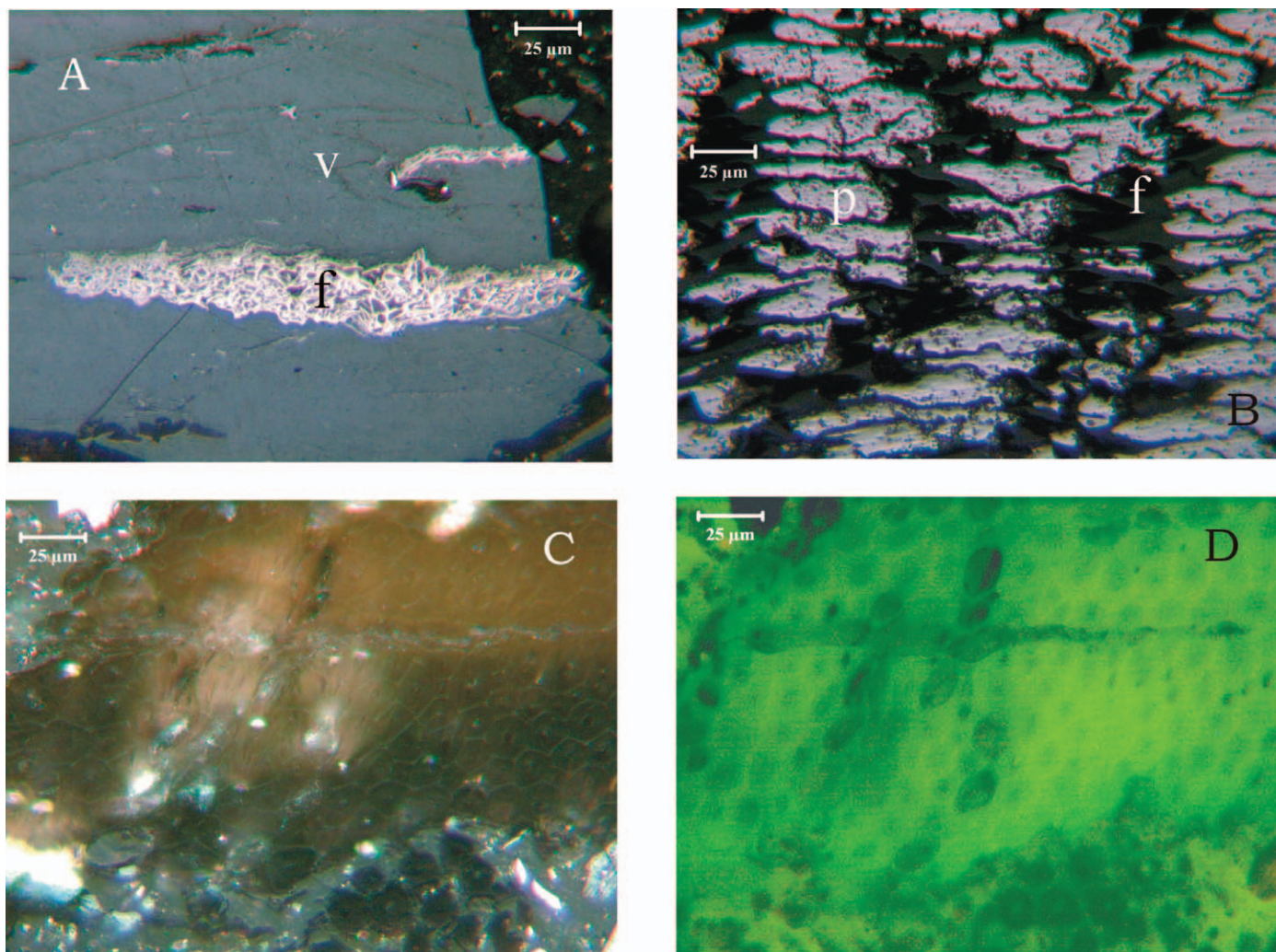
Fig. 1. (A) Fusinite (f) in vitrinite (v) in coal portion of fuel blend. (B) Pyrite (p) in fusinite (f) in coal portion of fuel blend. (C) Switchgrass in fuel blend (white-light illumination). (D) Switchgrass in fuel blend (blue-light illumination).

emissions, and the ability of CFBC to handle relatively coarse fuel (compared with, e.g., 85–90% <75-µm fuel for pulverized combustion) make biomass an attractive blend component.

Bed ash consists primarily of Ca (40–50% CaO) followed by S (>20% as SO_3) and silica (15–20% SiO_2) for both samplings, indicating that bed ash contains a significant amount of the limestone-derived fluidized bed. The fly ash chemistry is dominated by near-equal amounts of SiO_2 and CaO ($\approx$30%), with significant amounts of S (20% as SO_3; Table 1). The high CaO concentration in fly ash can also be attributed to the contribution of the limestone sorbent, as the fuel fired in both samplings is not particularly enriched in Ca. The fly ash samples are compositionally similar to high-Ca lignite-fired fly ash (Koukouzas et al., 2006; Izquierdo et al., 2011). However, given the mineralogical differences between pulverized-coal-combustion (PCC) fly ash and CFBC fly ash, the latter fly ashes cannot strictly be regarded as class C fly ash. Zinc and Mn, both minor constituents in limestone, are present in greater amounts in the fly ash and bed ash than in the coal + switchgrass feed; otherwise, the trace elements tend to be diluted in the fly ash and bed ash compared to the fuel.

One of the most distinctive features of FBC ash is the consistently low concentrations of most trace elements in comparison with PCC fly ash (e.g., Moreno et al., 2005), which can be up to a 10-fold difference. This is likely due to ash being diluted by the limestone sorbent. Only those elements present in the limestone, such as Rb, Sr, Mn, and Zn, are also present in both bed ash and fly ash in concentrations comparable to those of PCC fly ash, but still on the low side. It is worth pointing out that, while they can be texturally different and also differ in the major element contents, bed ash and fly ash are very similar in their concentrations of trace elements for each sampling.

3.3. Mineralogy

The minerals present in our CFBC ash samples are reported in Tables 2 and 3 and can be classified into three categories: primary or relict minerals (from the components of the parent coal or combustion fuel or from the limestone), secondary or combustion minerals (from phases that were formed during the combustion process), and ternary or weathering minerals (from material formed during hydration of the fly ash). Most of the CFBC fly ash particles are subangular shaped, but cenospheres and pleurospheres are also present in trace levels.

According to the XRD, FE-SEM, Raman spectroscopy, and HR-TEM results, the most common crystalline species in FBC coal fly ashes are anhydrite; anorthite and other plagioclase feldspars;

Table 2

Percentage (wt%) of crystalline phases as determined by X-ray diffraction

Sampling	Sample	Quartz	Hematite	Anhydrite	Mullite	Portlandite	Anorthite
2007	93550 Bed ash B	8.4	2.8	22.2	–	55.2	11.4
	93553 Fly ash B1 in	16.8	12.2	35.2	10.8	3.3	21.7
	93554 Fly ash B2 in	19.9	14.8	32.9	3.1	4.1	25.2
2010	93585 Bed ash B	15.2	3.0	49.6	12.3	12.4	7.5
	93588 Fly ash B1 in	44.2	8.9	28.1	1.9	2.0	15.0
	93589 Fly ash B2 in	37.0	7.3	20.6	15.0	8.8	11.3

gypsum; hematite; lime; magnetite; mullite; portlandite; quartz; and traces of alkali sulfates, calcium aluminate, calcium silicate, and Fe-Al spinels (Tables 2 and 3). These observations are in line with the findings of other authors, who reported the occurrence of low glass contents (<60%) and relatively high contents (2–30%) of quartz, illite, feldspars, anhydrite, and hematite/maghemite, with traces of lime, portlandite, gehlenite, magnesioferrite, silvite, periclase, rutile, and thenardite (Koukouzas et al., 2007, 2009; Izquierdo et al, 2008). The low combustion temperature (<900°C) may account for the low glass contents compared with PCC fly ash and for the presence of relict phases from coal such as illite or dolomite, although these, particularly the dolomite, are likely to be a contribution from the fluidizing bed. In general, XRD and

electron beam results indicated the CFBC fly ashes, compared with previously studied class F fly ash (e.g., Silva et al., 2010a,b), showed high contents of anhydrite, anorthite, and quartz and the lowest contents of hematite (Tables 2 and 3) due to the operational conditions of this coal combustion technology in the studied plants. The mineralogical composition of the studied ash samples is analogous to the assemblage observed in class C fly ash, e.g., combustion ashes from high-Ca lignite-fired stations, with high levels of quartz, feldspars, and a range of Ca-bearing species (Koukouzas et al., 2006; Izquierdo et al., 2011). In total, these observations underline the fact that the combustion technology and operational conditions have a significant impact on the ash mineralogy, in some cases more than the feed coal characteristics,

Table 3

Minerals and nanoparticles identified in the studied samples

	Bed ash (2007) 93550	Fly ash B1 in (2007) 93553	Fly ash B2 in (2007) 93554	Bed ash (2010) 93585	Fly ash B1 in (2010) 93588	Fly ash B2 in (2010) 93589
Hydr/oxides						
Anatase	b, c	b, c	c	c	b, c	c
Chromite		c			c	
Goethite	c	b, c	b, c	c	c	c
Hematite	a, b, c, d	b, c, d	c, d	c, d	c, d	c, d
Lime	a, b, c	a, b, c	a, b, c	a, b, c	a, b, c	a, b, c
Magnetite	c	c	b, c	c	b	b, c
Portlandite	d	d	d	d	d	d
Rutile	b, c	b, c	b, c	c	b, c	c
Silicates						
Anorthite	a, b, c	a, b	b	b	b, c	b, c
Akermanite			c, d			
Andradite			c		c	
Cristobalite	a, c	c	c	c	c	c
Illite	c, d	b, c, d	b	b, c, d	c, d	c, d
Diopside		c				c
Mullite		a, b, d	a, b, d	b, c, d	a, c, d	b, c, d
Muscovite	c		c	b, c	c	c
Pyrophyllite	c	c	c	c	b, c	b, c
Quartz	d	d	d	d	d	d
Sulfates						
Anhydrite	d	d	d	d	d	d
Barite	a, c	a, b, c	a, b, c	a, b, c	a, b, c	a, b, c
Gypsum	a	a	a, b	b	a, b	a, b
Jarosite	a, c	a, c	a, c	a, c	a, c	a, c
Schwertmannite	c	c	c	c	c	c
Carbonates						
Dolomite	a, b, c	a, b	b	b	b, c	b, c
Sulfides						
Galena	b				b	
Pyrrhotite	a, b, c	a, b, c	b, c	b, c	b	b
Amorphous	a, b, c, d	a, b, c, d	a, b, c, d	a, b, c, d	a, b, c, d	a, b, c, d

Note: Analytical methods: a = field emission–scanning electron microscopy (FE-SEM), b = Raman, c = high-resolution transmission electron microscope (HR-TEM), d = X-ray powder diffraction (XRD).
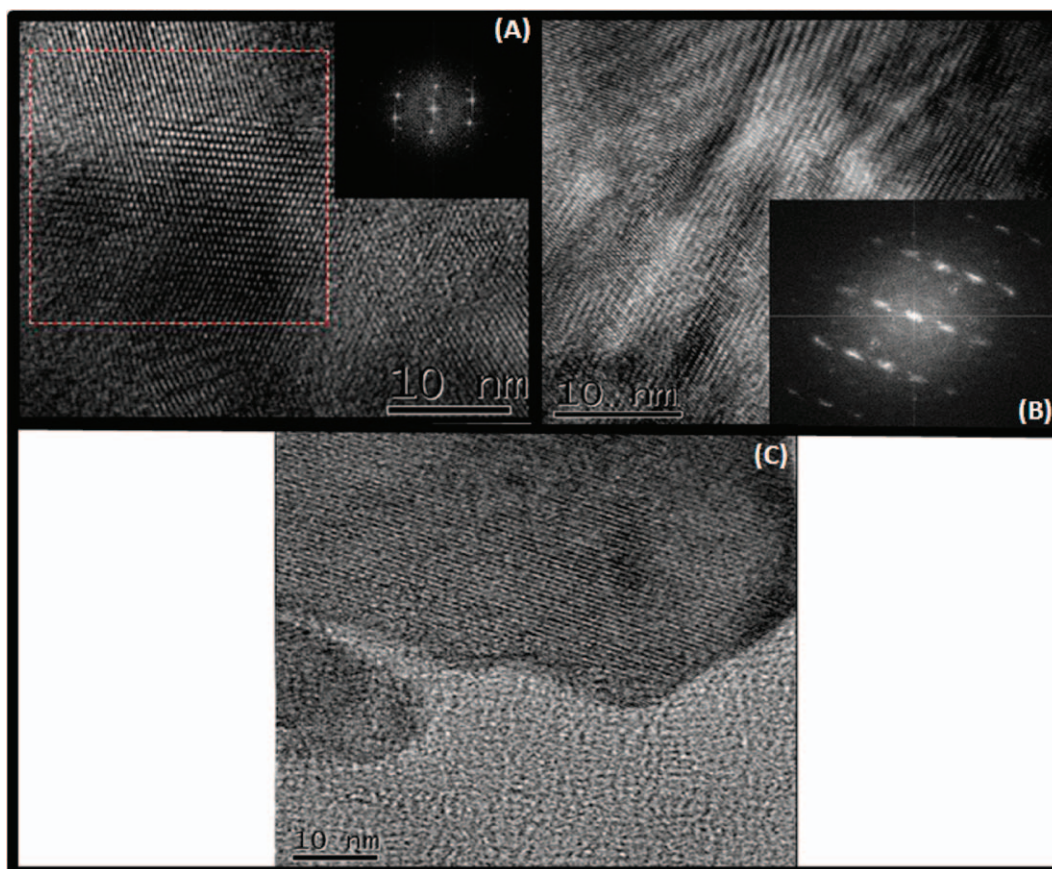
Fig. 2. High-resolution transmission electron microscope (HR-TEM) 93550 sample images with fast Fourier transform identification showing (A) anatase, (B) rutile, and (C) goethite.
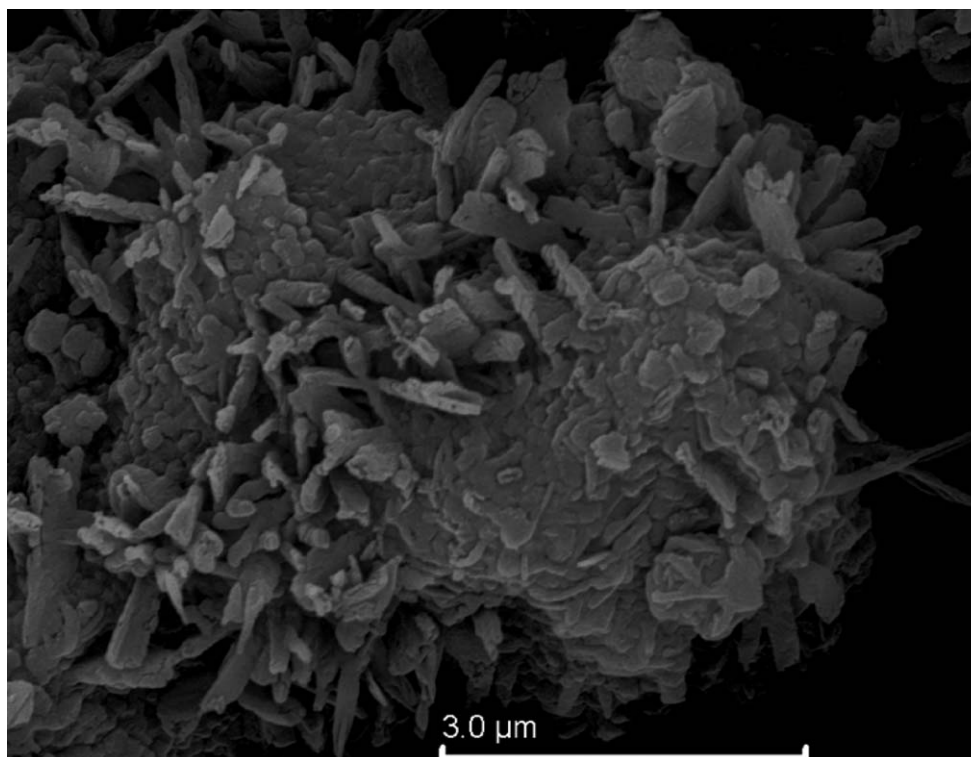

Fig. 3. Complex assemblage of anhydrite, bassanite, and gypsum.
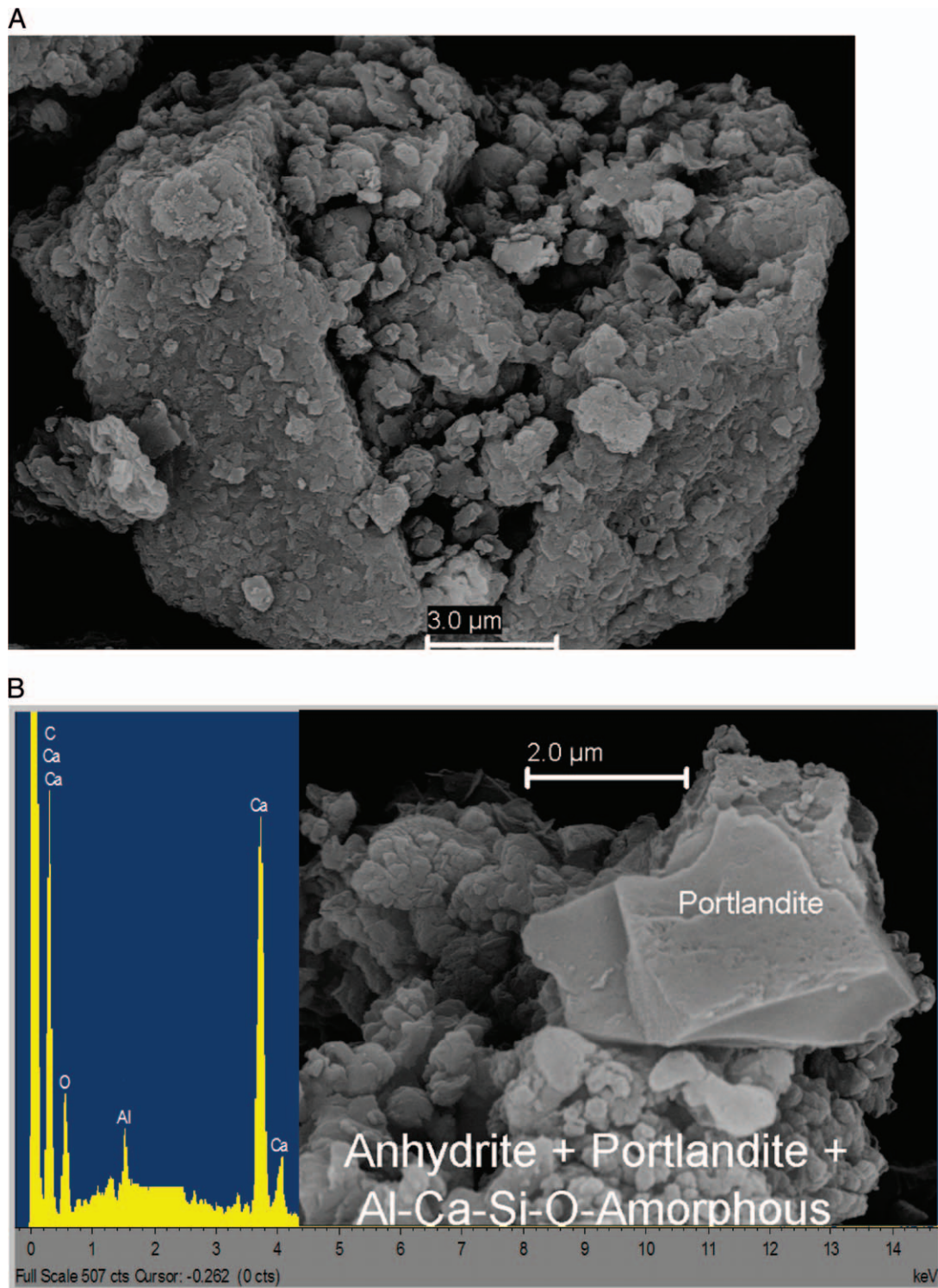
Fig. 4. (A) Complex assemblage of amorphous minerals and anorthite (angular and spherical assemblage). (B) Portlandite and amorphous Ca-phases.

although it is equally true that the mineral cannot be created if the raw ingredients are not present.

There are mineralogical differences between the ashes from the two samplings and between the two fly ash hoppers within each sampling time. The differences in the quartz content between the 2007 and 2010 fly ashes might be attributable to differences in the feed coal and in the limestone used for the fluidized bed. The differences in the proportions of anhydrite, mullite, portlandite, and anorthite could be a function of the coal and limestone chemistry or to other differences in the operating conditions of the CFBC combustor and the ash collection system. Similarly, the differences in the mullite and anorthite proportions between the B1 and B2 hopper fly ashes for both sampling times could be the result of subtle interactions in the flue gas chemistry, specifically in the SiO_2-Al_2O_3-CaO system. A controlled study of input fuel and carbonate chemistry, combustion conditions, and ash-collection conditions was beyond the scope of this investigation.
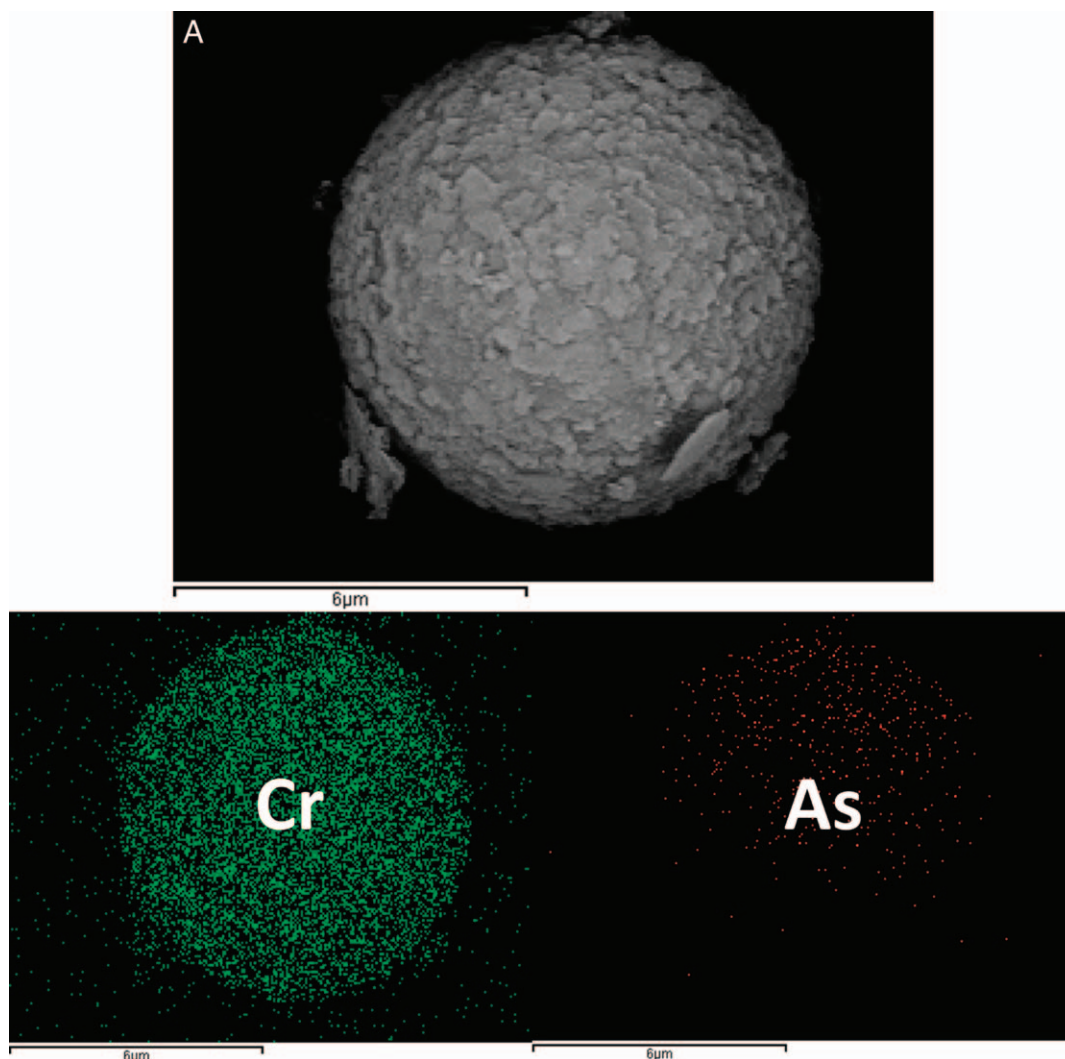
Fig. 5. (A) Spinel (hematite and minor proportions of magnetite) containing As (in red) and Cr (in green).

Typically, mullite occurs in coal fly ashes produced by the (co)-combustion of coal at temperatures $>1200°C$ (higher than CFBC temperatures) with an excess of Al_2O_3/SiO_2 in the Al-Si glass (Silva et al., 2010b). For our CFBC ash samples, the highest mullite contents (11–15%) were reported in samples 93553, 93585, and 93589 (Table 2). For the remaining CFBC fly ashes selected for this study, mullite occurs in proportions <4%. Calcium may also interact with aluminosilicate materials at the high temperatures associated with coal combustion to form a range of Ca-silicates, including anorthite, ackermanite, and diopside, as well as Ca-sulfates in minor proportions (e.g., anhydrite and gypsum). Most of the quartz crystals remain intact and are present as angular particles due to the relatively low temperature in the CFBC.

Significant amounts of anatase, barite, dolomite, magnesite, galena, goethite, gypsum, illite, jarosite, lime, pyrrhotite, muscovite, and rutile were detected (Table 3). Most of these minerals and associated amorphous materials were identified in the nanoscale by HR-TEM/SAED/EDS (e.g., anatase, Fe-sulfates, rutile, goethite; Figure 2) and contain hazardous elements (e.g., As, Cd, Cr, Hg, and Pb), especially in Fe- and Al-oxy/hydroxide.

The occurrence of anhydrite in the CFBC ashes is likely due to both the dehydration of bassanite and/or gypsum, easily detected by morphology and FE-SEM/EDS (Figure 3A) formed by the reaction of carbonates (i.e., calcite) and Fe-sulfides (i.e., pyrite, marcasite, chalcopyrite), and the reaction of organically bound Ca with gaseous SO_r. Anhydrite is present in all samples and is typically found as plate, needle, or wedge-shaped crystals. This species may react with water to form gypsum or ettringite, the latter of which is an undesirable mineral in cement or concrete production (Koukouzas et al., 2009).

FIB-SEM was used for HR-TEM preparation where the individual mineral nanoparticles were too small and/or not abundant enough to be reliably identified by XRD and/or Raman. The FIB-SEM platforms allow for both high-resolution imaging and sample preparation for HR-TEM. Thus, textures observed at the micron scale, such as chemical zonation and mineral nanoparticle replacement, can be linked to nanoscale features, such as polymorphism, polytypism, planar defects, or the occurrence of nanoparticles. Similar results were reported by Reich et al. (2011). Put into the mineral-deposit context, the observations by all analytical procedures presented in this work can constrain important processes such as incorporation and release of trace elements in CFBC ashes.

Figure 4 shows more complex multimineral phases present in CFBC ash. Figure 4A, observed by SEM after FIB preparation,
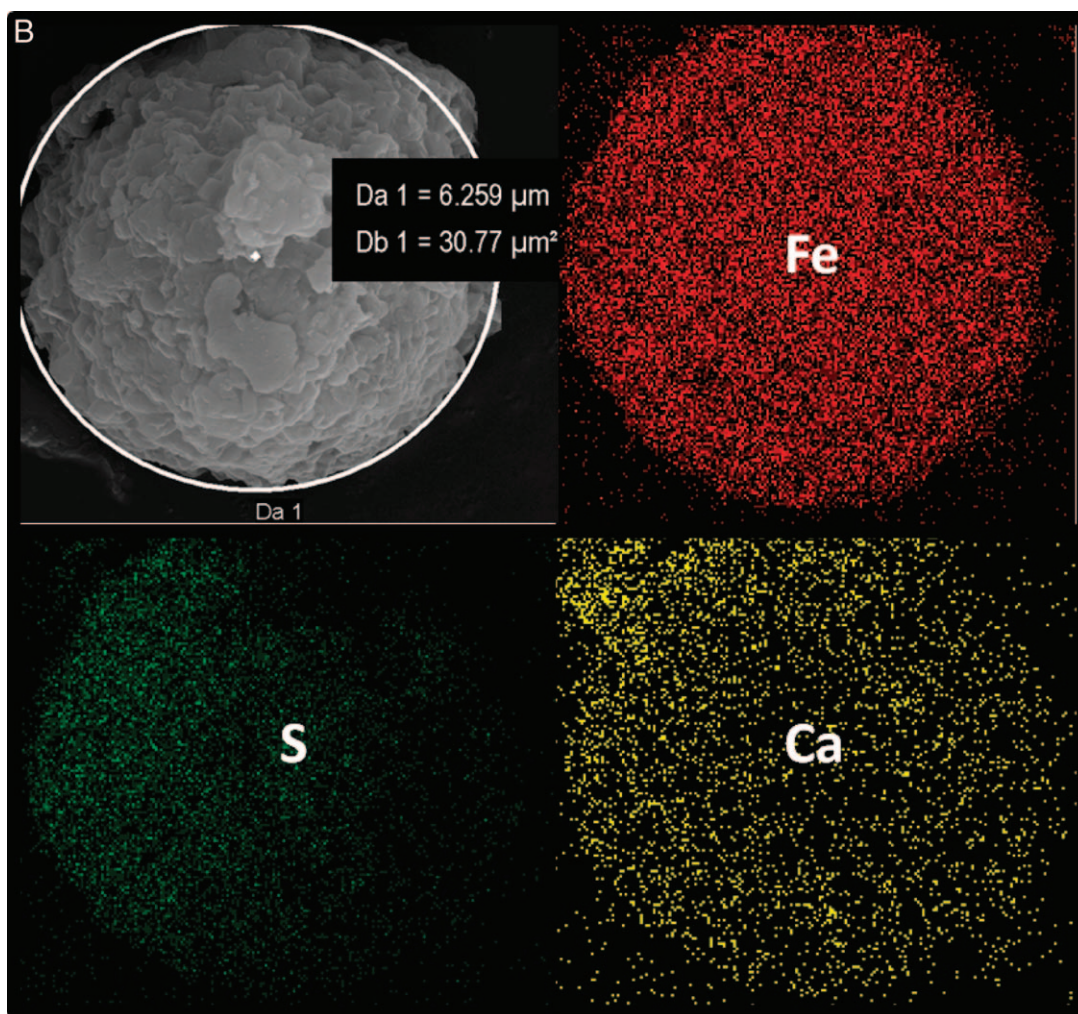
Fig. 5. (B) Complex spherical assemblage of hematite, magnetite, anhydrite, and Ca-O-S-amorphous minerals (element mapping: Fe in red; Ca in yellow; S in green).

shows an assemblage of amorphous ultrafine minerals and anorthite. In addition, Figure 4B represents a typical example of the interaction between portlandite and amorphous Ca-phases identified by FE-SEM/EDS in all of the studied ashes. These phases present complex semispherical and angular assemblages depending on combustion conditions and fuel utilized and were noted in previous works on CFBC ash (Armesto and Merino, 1999; Vuthaluru and Zhang, 2001).

All of the studied coal ashes contain several Fe-oxides, of which hematite is the most abundant (Table 2). Hematite can be formed by either oxidation of organically bound Fe in coal or Fe-bearing minerals, such as pyrite and siderite, during coal combustion processes. In general, hematite is usually considered to be a secondary mineral, since it can be formed by oxidation of pyrite or marcasite; decarbonation of siderite or ankerite; and secondary jarosite, or schwertmannite, or goethite reactions (Silva et al., 2011a,b,c). In the present study, other Fe-nanohydr/oxides (e.g., magnetite, goethite, among others shown on Table 3) were detected in the CFBC fly ashes, predominantly produced by the combustion-induced decomposition reactions of the sulfides and Fe-carbonate species present in the feed coal.

The spinel group, detected in minor portions, includes crystalline and nanohydr/oxides and encapsulated hazardous elements such as and Cr (Figure 5A). However, similar spherical assemblages containing several impurities (e.g., anhydrite and Ca-O-S-amorphous mineral nanoparticles) were not able to encapsulate hazardous elements (Figure 5B).

3.4. Solubility of elements

The pH of the leachates is strongly alkaline, with values consistently around 12.6 for the whole data set (Table 4). The ion balance revealed that much of the Ca in the leachates (14–25 g/kg leachable Ca) is largely unbalanced with the major anions determined (e.g., chlorides <200 mg/kg and sulfates around 1600 mg/kg), suggesting that the leachable Ca occurs primarily as $CaO/Ca(OH)_2$. This is supported by the mineralogical analysis discussed above and reported in Table 3, which confirmed the presence of lime and portlandite. Between 9% and 16% of the total Ca is water soluble, which is consistent with the range of water-extractable proportions measured for a large PCC fly ash data set (7–14%; Izquierdo et al., 2011, and references therein). Similar leachable concentrations of Ca and S were reported for lignite-derived fly ash (Izquierdo et al., 2011). Other elements typically occurring in readily soluble chlorides and sulfates, such as Na, K, Sr, and Cl, revealed variable leachable concentrations (up to 200 mg/kg).

The low overall mobility of metals is likely a result of decreasing solubility and enhanced adsorption processes with the increasing pH.

Table 4

Water leachable concentrations (mg/kg) of elements in bed ash and fly ash samples

	2007 sampling			2010 sampling		
	93550 Bed ash	93553 Fly ash B1 in	93557 Fly ash B2 in	93585 Bed ash	93588 Fly ash B1 in	93589 Fly ash B2 in
pH	12.7	12.7	12.7	12.7	12.7	12.7
F^-	0.4	2.3	2.2	0.6	1.7	1.6
Cl^-	<4	173	162	<4	152	156
NO_3^-	<2	<2	<2	<2	<2	<2
SO_4^{2-}	1576	1797	1637	1579	1572	1608
Al	<0.01	<0.01	<0.01	<0.01	<0.01	<0.01
As	0.3	0.3	0.4	0.4	0.3	0.2
B	1.6	6.3	6.6	0.7	0.6	0.2
Ba	1.3	3.9	3.9	2.2	4.3	1.9
Bi	<0.01	<0.01	<0.01	0.03	0.1	0.04
Ca	34,172	34,002	28,229	25,778	16,675	14,451
Cd	0.04	0.03	0.05	0.03	0.03	0.01
Ce	<0.01	<0.01	<0.01	0.0	<0.01	<0.01
Co	0.05	0.07	0.1	0.07	0.03	<0.01
Cr	0.2	1.0	1.0	0.3	1.7	0.7
Cu	<0.01	<0.01	<0.01	<0.01	<0.01	<0.01
Er	<0.01	<0.01	<0.01	<0.01	<0.01	<0.01
Fe	<0.01	<0.01	<0.01	<0.01	0.0	0.1
Ga	1.3	1.5	1.4	1.3	1.3	1.2
Ge	0.03	0.01	<0.01	<0.01	<0.01	0.03
K	52	19	22	84	56	44
Li	0.8	0.9	0.9	1.4	1.3	0.8
Mg	1.1	1.1	1.1	1.5	0.9	0.4
Mn	<0.01	<0.01	<0.01	<0.01	<0.01	<0.01
Mo	0.4	0.8	1.0	0.8	1.0	0.7
Na	7.3	7.7	6.7	8.8	6.3	3.1
Ni	0.1	0.1	0.1	0.1	0.1	0.1
P	<0.01	<0.01	0.03	0.05	<0.01	<0.01
Pb	0.2	<0.01	<0.01	<0.01	<0.01	0.2
Sb	0.1	0.1	<0.01	<0.01	0.04	0.04
Se	0.6	1.2	1.1	0.9	0.9	0.9
Si	1126	902	569	405	269	188
Sr	55	31	32	13	15	17
Ti	<0.01	<0.01	<0.01	<0.01	<0.01	<0.01
Tl	<0.01	<0.01	0.4	<0,001	0.1	<0.01
V	0.1	<0.01	<0.01	<0.01	<0.01	<0.01
W	0.2	0.2	0.2	0.2	0.2	0.1
Zn	0.02	0.12	0.13	0.07	0.07	0.02

Several environmentally sensitive trace elements (i.e., Bi, Cd, Co, Cu, Ge, Ni, rare earth elements [REEs], Sb, Tl, V, and Zn) were found to be poorly soluble and revealed leachable concentrations <0.1 mg/kg. Cadmium, Pb, Cu, Ni, Co, and Zn have been occasionally reported to show amphoteric behavior in PCC fly ash, with their solubility sharply increasing with pH >11.5 as a result of the formation of more soluble anionic hydroxo complexes. However, the studied ash samples were not consistent with this leaching pattern, and the mentioned metals remained immobile.

Elements likely to form oxyanionic species, i.e., As, Cr, Sb, Se, V, and W, are regarded as the main concern in PCC fly ash due to high pH enhancing their mobility. This is in agreement with the results of FE-SEM and HR-TEM because these elements occurred mainly as amorphous phases with minor phases in Al-Si-K-Mg-P-spheres. Therefore, by not possessing well-defined crystal structures, they are easily leachable at pH 8–12. The studied ash samples revealed leachable concentrations <0.5 mg/kg for As, Sb, V, and W, while Cr, Mo, and Se showed variable leachability between 0.4 and 1.2 mg/kg. These values tend to be in the lower range of PCC fly ash (Izquierdo et al., 2011) and are not of major concern. A number of processes can contribute to attenuate

oxyanionic leaching in the studied ash samples. For example, the large amounts of Ca in solution may promote the precipitation of Ca-bearing salts, thus removing elements from solution. The formation of Ca-arsenate is common in Ca-rich ash (Yudovich and Ketris, 2005), while V leaching was found to be delayed in the presence of large amounts of Ca (Querol et al., 2001). In addition, the formation of ettringite at pH >11.5 is acknowledged as a major scavenger for species structurally similar to sulfate, e.g., arsenates, chromates, selenates, and vanadates, among others, or likely to be adsorbed onto already formed ettringite (Hassett et al., 2005; Cornelis et al., 2008).

4. Summary

The bed ash (spent bed) and fly ash from a Kentucky coal-fired 268 MW CFBC were sampled in 2007 and 2010. The second sampling represented a time when biomass (switchgrass *Panicum virgatum*) represented up to about 10% of the fuel. The exact amount of biomass in the fuel blend represented by the ashes could not be quantified.

The major conclusions are as follows:

- The coal + switchgrass blend had a higher moisture and lower heating value than the coal-only fuel.
- Aside from the substitution of biomass for coal, changes in the coal and limestone supplies between the two sampling times complicate strict comparisons of the bed ash and fly ash chemistry of the two sample sets.
- The bed ash is dominated by CaO and SO_3, followed by SiO_2, and the fly ash has high CaO concentrations. While the fly ash superficially resembles fly ash from pulverized-fuel (pf) combustion of high-Ca lignites, the mineralogical differences imposed by the lower combustion temperatures in CFBC compared with pf combustion mitigate against consideration of the CFBC fly ash as a class C ash.
- The bed ash mineralogy is dominated by anhydrite, mullite (in the 2010 sample), portlandite, and anorthite. The fly ash has less portlandite and more anorthite than the bed ash. Variations in bed ash and fly ash mineralogy might be attributable to (known) changes in the fuel and limestone supply, as well as to changes in operating conditions between the sampling times.
- Other than more calcium in the 2007 sampling and consequently more leachable calcium, the majority of elements have leachable concentrations of the same order of magnitude and, in some cases, surprisingly similar values regardless of changes in the feed coal in between.

Acknowledgments

References

Armesto, L., Merino, J.L., 1999. Characterization of some coal combustion solid residues. Fuel 78, 613–618.

Basu, P., 1999. Combustion of coal in circulating fluidized-bed boilers: a review. Chemical Engineering Science 54, 5547–5557.

Basu, P., Fraser, S.A., 1991. Circulating fluidized bed boilers—design and operations. Butterworth-Heineman, Stoneham, MA, chap. 4, pp. 95–126.

Chen, J., Lu, X., 2007. Progress of petroleum coke combusting in circulating fluidized bed boilers—a review and future perspectives. Resources, Conservation and Recycling 49, 203–216.

Cornelis, G., Johnson, C.A., Gerven, T.V., Vandecasteele, C., 2008. Leaching mechanisms of oxyanionic metalloid and metal species in alkaline solid wastes: a review. Applied Geochemistry 23, 955–976.

Cui, H., Grace, J.R., 2007. Fluidization of biomass particles: a review of experimental multiphase flow aspects. Chemical Engineering Science 62, 45–55.

European Committee for Standardisation, 2002. Characterisation of Waste. Leaching—Compliance Test for Leaching of Granular Waste Materials and Sludges—Part 2: One Stage Batch Test at a Liquid to Solid Ratio of 10 L/kg for Materials with Particle Size below 4 mm. European Committee for Standardisation Report EN 12457-2:2002.

Giannuzzi, L.A., Prenitzer, B.I., Drown-Macdonald, J.L., Shofner, T.L., Brown, S.R., Irwin, R.B., Stevie, F.A., 1999. Electron microscopy sample preparation for the biological and physical sciences using focused ion beams. Journal of Process Analytical Chemistry 4, 162–167.

Hassett, D.J., Pflughoeft-Hassett, D.F., Heebink, L.V., 2005. Leaching of CCBs: observations from over 25 years of research. Fuel 84, 1378–1383.

Hower, J.C., Robertson, J.D., Thomas, G.A., Wong, A.S., Schram, W.H., Graham, U.M., Rathbone, R.F., Robl, T.L., 1996. Characterization of fly ash from Kentucky power plants. Fuel 75, 403–411.

Hower, J.C., Robl, T.L., Anderson, C., Thomas, G.A., Sakulpitakphon, T., Mardon, S.M., Clark, W.L., 2005. Characteristics of coal utilization products (CUBs) from Kentucky power plants, with emphasis on mercury content. Fuel 84, 1338–1350.

Hower, J.C., Robl, T.L., Thomas, G.A., 1999a. Changes in the quality of coal combustion by-products produced by Kentucky power plants, 1978 to 1997: consequences of Clean Air Act directives. Fuel 78, 701–712.

Hower, J.C., Robl, T.L., Thomas, G.A., 1999b. Changes in the quality of coal delivered to Kentucky power plants, 1978 to 1997: responses to Clean Air Act directives. International Journal of Coal Geology 41, 125–155.

Hower, J.C., Robl, T.L., Thomas, G.A., Hopps, S.D., Grider, M., 2009. Chemistry of coal and coal combustion products from Kentucky power plants: results from the 2007 sampling, with emphasis on selenium. Coal Combustion & Gasification Products 1, 50–62. http://www.coalcgp-journal.org/papers/2009/CCGP-D-09-00013-Hower-supp.pdf

Izquierdo, M., Koukouzas, N., Touliou, S., Panopoulos, K.D., Querol, X., Itskos, G., 2011. Geochemical controls on trace element leaching from lignite-fired by-products. Applied Geochemistry 26, 1599–1606.

Izquierdo, M., Moreno, N., Font, O., Querol, X., Alvarez, E., Antenucci, D., Nugteren, H., Luna, Y., Fernández-Pereira, C., 2008. Influence of the co-firing on the leaching of trace pollutants from coal fly ash. Fuel 87, 1958–1966.

Kitto, J.B., Stultz, S.C., 2005. Steam: Its Generation and Use, 41st ed. Babcock & Wilcox, Barberton, OH, chap. 17.

Koukouzas, N.K., Hämäläinen, J., Papanikolaou, D., Tourunen, A., Jantti, T., 2007. Mineralogical and elemental composition of fly ash from pilot scale fluidized bed combustion of lignite, bituminous coal, wood chips and their blends. Fuel 86, 2186–2193.

Koukouzas, N.K., Ward, C.W., Papanikolaou, D., Li, Z., Ketikidis, C., 2009. Quantitative evaluation of minerals in fly ashes of biomass, coal and biomass–coal mixture derived from circulating fluidised bed combustion technology. Journal of Hazardous Materials 169, 100–107.

Koukouzas, N.K., Zeng, R., Perdikatsis, V., Xu, W., Kakaras, E., 2006. Mineralogy and geochemistry of Greek and Chinese coal fly ash. Fuel 85, 2301–2309.

Meier, A.L., Lichte, F.E., Briggs, P.H., Bullock, J.L., 1996. Analysis of coal ash by inductively coupled plasma emission spectroscopy and inductively coupled plasma–mass spectroscopy. In: Analytical Methods Manual for the Mineral Resource Surveys Program, US Geological Survey (Arbogast, B.F., ed.). U.S. Geological Survey Open-File 96-525, pp. 109–125.

Moreno, N., Querol, X., Andrés, J.M., Stanton, K., Towler, M., Nugteren, H., Janssen-Jurkovicová, M., Jones, R., 2005. Physico-chemical characteristics of European pulverized coal combustion fly ashes. Fuel 84, 1351–1363.

Oliveira, M.L.S., Ward, C.R., French, D., Hower, J.C., Querol, X., Silva, L.F.O., 2012. Mineralogy and leaching characteristics of beneficiated coal products from Santa Catarina, Brazil. International Journal of Coal Geology 94, 314–325.

Querol, X., Umaña, J.C., Alastuey, A., Ayora, C., Lopez-Soler, A., Plana, F., 2001. Extraction of soluble major and trace elements from fly ash in open and closed leaching systems. Fuel 80, 801–813.

Querol, X., Whateley, M.K.G., Fernandez-Turiel, J.L., Tuncali, E., 1997. Geological controls on the mineralogy and geochemistry of the Beypazari lignite, central Anatolia, Turkey. International Journal of Coal Geology 33, 255–271.

Quispe, D., Pérez-López, R., Silva, L.F.O., Nieto, J.M., 2012. Changes in mobility of hazardous elements during coal combustion in Santa Catarina power plant (Brazil). Fuel 94, 495–503.

Reich, M., Hough, R.M., Deditius, A., Utsunomiya, S., Ciobanu, C.L., Cook, N.J., 2011. Nanogeoscience in ore systems research: principles, methods, and applications: Introduction and preface to the special issue. Ore Geology Reviews 42, 1–5.

Ribeiro, J., Flores, D., Ward, C.R., Silva, L.F.O., 2010. Identification of nanominerals and nanoparticles in burning coal waste piles from Portugal. Science of the Total Environment 408, 6032–6041.

Silva, L.F.O., da Boit, K.M., Oliveira, M.L.S., Hower, J.C., 2010a. Fullerenes and metallofullerenes in coal-fired stoker fly ash. Coal Combustion and Gasification Products 2, 1–11.

Silva, L.F.O., Oliveira, M.L.S., Neace, E.R., O'Keefe, J.M.K., Henke, K.R., Hower J.C., 2011a. Nanominerals and ultrafine particles in sublimates from the Ruth Mullins coal fire, Perry County, Eastern Kentucky, USA. International Journal of Coal Geology 85, 237–245.

Silva, L.F.O., Oliveira, M.L.S., Philippi, V., Serra, C., Dai, S., Xue, W., Chen, W., O'Keefe, J.M.K., Romanek, C.S., Hopps, S.G., Hower, J.C., 2011b. Geochemistry of carbon nanotube assemblages in coal fire soot, Ruth Mullins fire, Perry County, Kentucky. International Journal of Coal Geology 94, 206–213.

Silva, L.F.O., Querol, X., da Boit, K.M., Fdez-Ortiz deVallejuelo, S., Madariaga, J.M., 2011c. Brazilian coal mining residues and sulphide oxidation by

Fenton's reaction: an accelerated weathering procedure to evaluate possible environmental impact. Journal of Hazardous Materials 186, 516–525.

Silva, L.F.O., Sampaio, C.H., Guedes, A., Fdez-Ortiz de Vallejuelo, S., Madariaga, J.M., 2012. Multianalytical approaches to the characterisation of minerals associated with coals and the diagnosis of their potential risk by using combined instrumental microspectroscopic techniques and thermodynamic speciation. Fuel 94, 52–63.

Silva, L.F.O., Ward, C.R., Hower, J.C., Izquierdo, M., Waanders, F.B., Oliveira, M.L.S., Li, Z., Hatch, R., Querol, X., 2010b. Mineralogy and leaching characteristics of coal ash from a major Brazilian power plant. Coal Combustion and Gasification Products 2, 51–65.

Treff, P., Johnson, C., 2005. Clean power from coal: design and status of East Kentucky Power Cooperative's E.A. Gilbert unit. In: Proceedings of the 18th International Conference of Fluidized Bed Combustion, 2005, Toronto, Canada, 22–25 May 2005, Article No. FBC2005-78106. American Society of Mechanical Engineers, Toronto, pp. 121–126.

U.S. Department of Energy, Energy Information Administration, 2010. Summary statistics for the United States. http://www.eia.doe.gov/electricity/epa/epates. html, accessed 21 May 2014.

U.S. Environmental Protection Agency (US EPA), 2010. Controlling power plant emissions: chronology. http://www.epa.gov/hg/control_emissions/decision. htm, accessed 21 May 2014.

U.S. Environmental Protection Agency (US EPA), 2011. National emission standards for hazardous air pollutants from coal- and oil-fired electric utility steam generating units and standards of performance for electric utility steam generating units. http://yosemite.epa.gov/opei/rulegate.nsf/byRIN/2060-AP52#4, accessed 21 May 2014.

Van de Velden, M., Baeyens, J., Dougan, B., McMurdo, A., 2007. Investigation of operational parameters for an industrial CFB combustor of coal, biomass and sludge. China Particuology 5, 247–254.

Vuthaluru, H.B., Zhang, D., 2001. Effect of Ca- and Mg-bearing minerals on particle agglomeration defluidisation during fluidised-bed combustion of a South Australian lignite. Fuel Processing Technology 69, 13–27.

Wheeler, P.A., Patel, N.M., Painter, A., 1995. Fluidised bed combustion of municipal solid waste. Proceedings of the International Conference on Fluidized Bed Combustion 1, 597–607.

Yudovich, Ya.E., Ketris, M.P., 2005. Arsenic in coal: a review. International Journal of Coal Geology 61, 141–196.